

## Distribution of sodium and chlorine in samples of Egyptian pyramids

Guy Demortier\*

*Emeritus professor of physics, University of Namur (Belgium)*

### Abstract

Concentrations of light elements using micro-PIXE and micro-PIGE reveal the elemental composition of the various materials used for the construction of the pyramids. Light elements (mainly Na, Cl and S) show a very heterogeneous distribution for the pyramid's material in contrast with the extremely homogeneous distribution of these elements in natural limestone from quarries of Turah and Maadi and the bedrock of Saqqarah. The micro-PIXE elemental maps present new evidence for the application of a molding procedure.

**Keywords:** Egyptian pyramids, geopolymer, inclusions, micro-PIXE, natron. © 2020 Geopolymer Institute. All rights reserved.

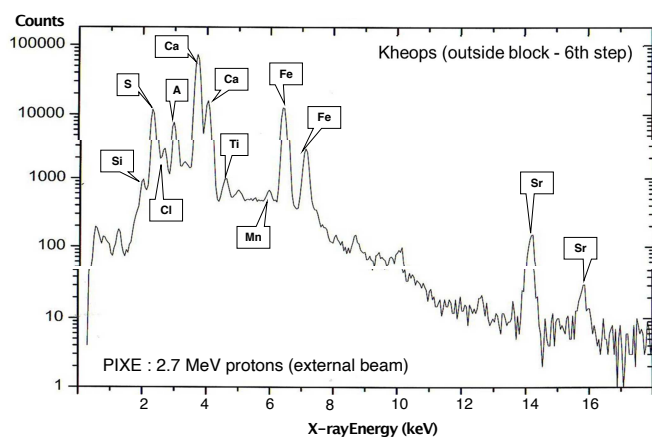


Figure 1: PIXE spectrum of a sample collected at Khufu pyramid outside block - 6th step

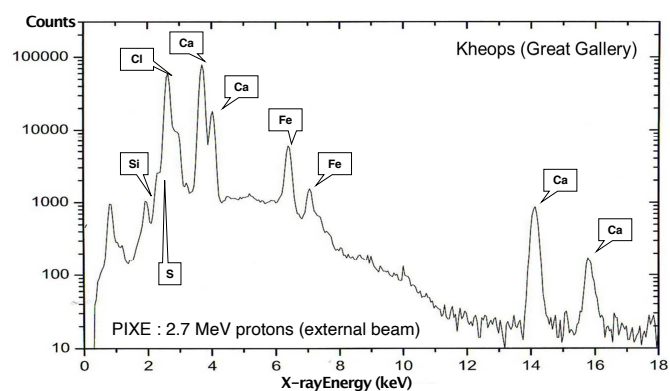


Figure 2: PIXE spectrum of a sample collected at the Great Gallery of the Khufu pyramid.

### 1. Introduction

The study of the composition of the blocks of the Egyptian pyramids using PIXE and PIGE was undertaken on 3 samples (only!) about 25 years ago at LARN (University of Namur - Belgium) and the results have been published in 2004 (Demortier, 2004). Surprisingly the concentration of light elements (F, Na, Mg, Al, Si) determined with PIGE in one of these samples was much too high to conclude that it was natural limestone exclusively. Nuclear magnetic resonance spectroscopy of  $^{27}\text{Al}$  and  $^{29}\text{Si}$  on these samples indicated that they could have been produced in a basic liquid phase of high pH (around 10) (Demortier, 2004). These ion beam analyses and NMR results are in line with the proposal of Davidovits who suggested that the pyramids were cast in situ using granular limestone

aggregate, natron (a naturally occurring mixture of hydrated sodium carbonate:  $\text{Na}_2\text{CO}_3 \cdot 10\text{H}_2\text{O}$  with some sodium chloride and sodium sulfate), lime (probably produced by the combustion of wood in domestic fires) and water to produce an alkali aluminosilicate-based binder (Davidovits, 1986; Davidovits & Morris, 1988).

A large amount of S and Cl (several %) was also detected by PIXE in about 10 additional samples using the 2.7 MeV external proton beam of CEDAD (Lecce) (see Figure 1 and Figure 2): an additional reason to think that the huge blocks were not pure limestone (Demortier et al., 2008; Demortier, 2009). These results are in agreement with those of Barsoum *et al.* (Barsoum et al., 2006; MacKenzie K. J. D. et al., 2011) (using scanning and transmission electron microscopy and NMR analysis of pyramid's material and limestone samples collected in their vicinity) who states:

*“that the blocks of the pyramids contain micro-constituents with appreciable amount of silicon in combination with elements, such as*

Ca and Mg, in ratios that do not exist in any of the potential limestone sources. The intimate proximity of these micro-constituents suggests that at some time these elements had been together in a solution. Furthermore, between the natural limestone aggregates, the micro-constituents with chemistries reminiscent of calcite and dolomite which are not known to hydrate in nature were hydrated. The ubiquity of Si and the presence of submicron silica-based spheres in some of their micrographs strongly suggest that the solution was basic (pH 10 to 11). Transmission electron microscopy confirmed that some of these Si-containing micro-constituents were either amorphous or nano-crystalline, which is consistent with a relatively rapid precipitation reaction”.

As pointed out by Barsoum the investigation of the material at microscopic level would offer the way to differentiate natural limestone from man-made material. PIXE analyses with a proton microprobe were then undertaken on a larger number of samples: 35 from the Giza pyramids and 15 from limestone quarries located in Belgium, Hungary and three sites located close to the Giza plateau: Maadi, Turah and Saqqarah.

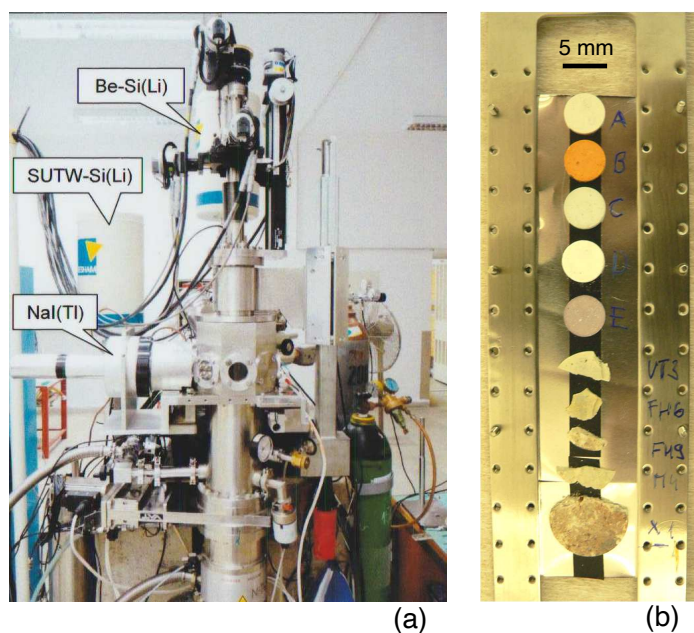


Figure 3: Oxford Microbeams-type SPM facility of Atomki (a) equipped with light and heavy element (super ultra-thin/Be-windowed) Si(Li) x-ray detectors as well as a NaI(Tl) gamma-ray detector. (b) Sample holder with polished pellets of reference and pyramid samples.

## 2. Micro-PIXE and micro-PIGE analyses

Analytical investigations were carried out at the scanning proton microprobe configuration of the Institute for

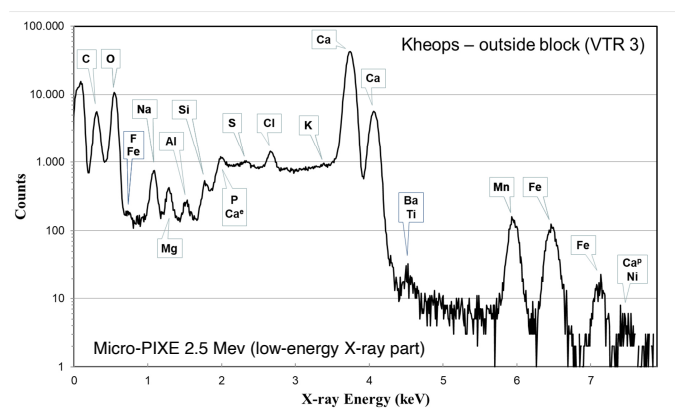


Figure 4: Micro-PIXE spectrum of a sample (vtr3) from the outside block of pyramid Khufu measured by the light element detector. The concentrations of major and some minor element are listed in Table 1. Other detected trace element: Mn=0.77 %.  $Ca^e$  and  $Ca^p$  are escape and pile-up peaks of calcium.

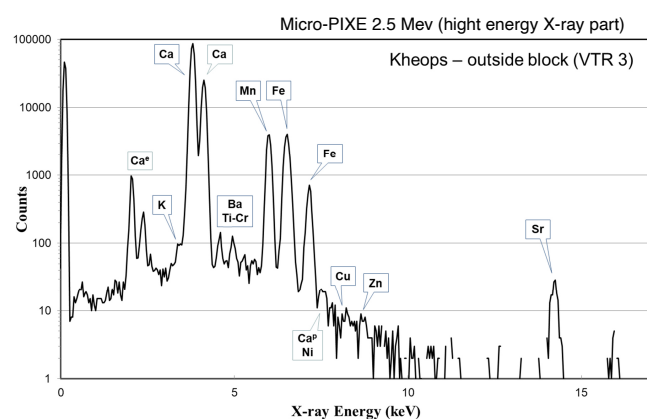


Figure 5: Micro-PIXE spectra of a sample (vtr3) from the outside block of pyramid Khufu measured by the light element detector. The concentrations of major and some minor element are listed in Table 1. Other detected trace elements: Mn/Ba/Sr=0.77 %/0.09 %/0.05 %;  $Ca^e$  and  $Ca^p$  are escape and pile-up peaks of calcium.

Nuclear Research, Hungarian Academy of Sciences (Debrecen) (Figure 3a) using advanced micro-PIXE and PIGE techniques (Szabó & Borbély-Kiss, 1993; Rajta et al., 1996; Uzonyi et al., 2001). The system is based on the 5 MV Van de Graaff generator of the institute (MTA Atomki). Concerning the operational principle of proton microprobes as well as the general features of ion beam analytical methods we refer to the literature, see e.g. (Grime et al., 1991; Demortier, 1995; Koltay et al., 2011; Grime, 2017).

The micro-PIXE experimental setup consisted of a super ultra-thin windowed (SUTW) Si(Li) X-ray detector and a Be windowed one which were operated simultaneously allowing the efficient detection of light elements down to carbon (in the 0.28-8 keV range) (Figure 4) as well as heavier ones (from K upwards), respectively (Figure 5) (Uzonyi et al., 2001). The SUTW detector was protected from backscattered particles with a permanent magnetic unit. In the case of the Be windowed detector

high solid angle ( $\sim 100$  msr) was assured and the intense soft characteristic x-rays ( $< 3$  keV) of low atomic number elements were attenuated with a Kapton® filter of  $375 \mu\text{m}$  thickness placed in front of the x-ray detector.

Characteristic X-ray spectra of samples were evaluated by the PIXEKLM-TPI (Atomki) program package. Using this software, the K, L (and M) characteristic lines of elements from carbon K-alpha upwards as well as their escape and pile-up peaks present in the spectra are fitted. The elemental concentrations are calculated from the  $K\alpha$  or  $L\alpha$  x-ray peak areas by the following formula: concentration = x-ray peak area/sensitivity factor. The sensitivity factors are derived from fundamental as well as experimental parameters (ECPSSR cross section for protons, fluorescence yields, transition probabilities, mass absorption coefficients, solid angle, x-ray absorbers, accumulated charge, proton energy, sample thickness, etc.) considering both absorption and enhancement effects as described in references (Szabó & Borbély-Kiss, 1993; Uzonyi & Szabó, 2005). It is mentioned that, except fluorine, PIXE provides quite low and acceptable detection limits for trace elements. Namely, in this case, the strong overlap between fluorine K-alpha and Fe L-alpha peaks as well as the relatively high background arising from light elements such as Na, Si, Cl, etc. can significantly increase the detection limit for F.

Previous experimental investigations (Demortier, 2004) have shown that PIGE technique can be a sensitive method for fluorine detection when the high energy gamma lines from the  $^{19}\text{F}(p,\alpha\gamma)^{16}\text{O}$  nuclear reaction ( $E_\gamma=6.129, 6.915$  and  $7.115$  MeV) are used for quantification. Namely, their intensities are an order of magnitude higher as compared to those of  $^{19}\text{F}(p, p'\alpha)^{19}\text{F}$  processes ( $E_\gamma=110, 197$  keV). Furthermore, these high energy peaks are relatively free from background and overlap with other elements (Kiss et al., 1985). In our experiment, the micro-PIGE setup consisted of a NaI(Tl) detector (diam=110 mm, solid angle  $\sim 0.8$  sr) placed at 90 degrees position to the direction of the beam and a lead shield of 1 cm thickness was applied. Concentrations were calculated from net gamma-ray peak areas normalized to accumulated charges. Calibration was based on the NIST 610 SRM as well as some home-made fluorine standards (Figure 6).

The microprobe was operated with a proton beam of 2.5 MeV energy in order to provide acceptable excitation conditions for both PIXE (C..Pb) and PIGE (F). The proton beam was focussed to a spot size of  $\sim 3 \mu\text{m}$ . The beam current was  $\sim 100$ -200 pA, the maximum scan size was  $1 \times 1$  mm<sup>2</sup>, the measurement times were typically  $\sim 600$ -900 s corresponding to relatively low  $\sim 0.1$ -0.2  $\mu\text{C}$  accumulated charges.

The whole measurement procedure has been calibrated and tested thoroughly by standard reference materials *e.g.* NIST 610, "Corning D" archaeological glass (Hoskin, 1999) (Wagner et al., 2012) and some home-made ones, as well as pure chemical compounds such as quartz, NaCl, etc for many times. On the average 3-15 rel. % accuracy can be achieved for the concentrations of major and minor

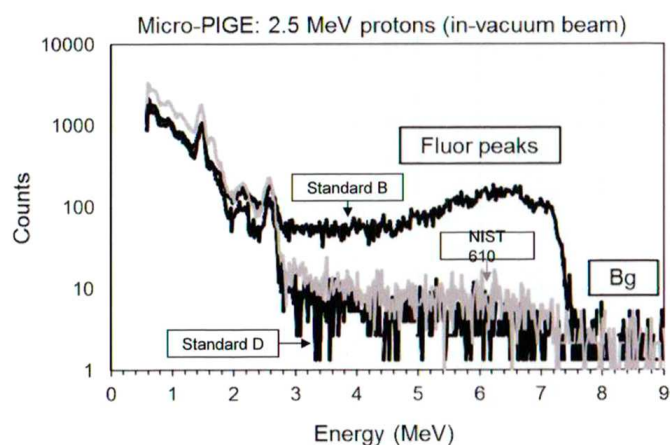


Figure 6: Micro PIGE spectrum of NIST610 SRM as well as two home-made standard samples. F=3.5 % (standard B), 0.03 % (NIST 610), 0 % (standard D). Counts were integrated for the  $E_\gamma=6.129, 6.915$  and  $7.115$  MeV lines as well as their single and double escape peaks in the 4.7-7.3 MeV energy region. Background was counted in 7.7-8.9 MeV interval.

elements and 5-20 rel. % for the trace elements as best values.

The detected elements in the PIXE spectra were quantified from carbon upwards lead. The elemental analysis (C, O, F, Na, Mg, Al, Si, P, S, Cl, K, Ca, Mn, Fe and Sr) results is given in Table 1 for a selection of the pyramid and quarries samples. These data refer to the mean values of 3 to 7 measurements on each sample. Other elements like Ti, Cr, Ni, Cu, Zn, and Ba were also observed.

### 3. Micro-PIXE results

The composition of the samples from pyramids and limestone's quarries obtained by PIXE in the proton microprobe configuration are reported in Table 2. The elemental concentrations are converted in the most probable oxide compounds.

We have selected only 6 elements (C, O, Na, S, Cl and Ca) in the following discussion of the distribution maps, but maps of F, Mg, Al, Si, P, K, Fe were simultaneously collected in the X-ray detectors, Fluor was also detected by PIGE technique only in a few samples. Future research is needed to clarify its role in various geochemical processes.

About 100 series of concentration maps of these elements were collected with a spatial resolution of  $5 \mu\text{m}$  to scan  $1 \text{ mm}^2$  on flat surfaces of polished pellets (Fig. 3b). They are taken in the internal part of fractured chunks of the pyramids (in order to avoid any external contamination) for comparison with natural limestone extracted from various quarries of Belgium, Hungary and Egypt (Maadi, Turah and Saqqarah).

Samples from Maadi quarry (maps in Figure 7) are very homogeneous: they contain mostly pure limestone with sometimes inclusions of aluminum, silicon and iron oxides, and traces of sodium, chlorine and sulfur with no

Table 1

	Maadi	Turah	Saqqarah	Pi Khufu	VTRS Khufu	FH123 Khufu	VT3 Khufu	FH7 Khufu	X1 Khufu
<b>C</b>	5,1	0,81	5,08	6,08	8,4	9,11	7,45	0,33	3,6
<b>O</b>	49,7	49,9	49,2	50,22	46,15	47,3	46,9	51,75	45,45
<b>F</b>		0,32	0,31		0,14	0,31	0,09	0,19	0,05
<b>Na</b>	0,32	0,14	0,45	0,19	<b>2,46</b>	<b>1,55</b>	<b>0,96</b>	<b>1,73</b>	<b>2,59</b>
<b>Mg</b>	0,56	0,73	0,4	0,61	0,5	0,72	0,39	0,67	0,62
<b>Al</b>	0,92	0,14		0,68	0,23	0,81	0,06	1,14	3,15
<b>Si</b>	2,06	0,29	1,05	1,68	2,58	2,36	0,16	2,93	6,04
<b>P</b>	0,16	0,11	0,09	0,07	0,04	0,02	0,18	0,09	0,12
<b>S</b>	0,06		0,02	0,43	0,07	0,28	0,18	15,9	<b>14,6</b>
<b>Cl</b>	0,06	0,06	0,24	0,02	<b>0,95</b>	<b>0,82</b>	<b>0,46</b>	<b>1,21</b>	<b>1,54</b>
<b>K</b>	0,1		0,09	0,08	0,15	0,11	0,05	0,26	0,46
<b>Ca</b>	40,2	40,26	42,5	38,7	38,07	36,19	41,6	23,17	19,34
<b>Ti</b>	0,05		0,02	0,03	0,01	0,04		0,06	0,21
<b>Mn</b>	0,01		0,01	0,03			0,74	0,01	0,06
<b>Fe</b>	0,51	0,1	0,29	0,65	0,06	0,03	0,64	0,65	2,05
<b>Sr</b>	0,12	0,18	0,22	0,08	0,26	0,18	0,05	0,04	0,14

Table 1: Elemental composition (16 elements) in selected quarries and pyramid's samples.

specific structure. Similar maps have been collected for samples of Turah quarry, bedrock of Saqqarah but also for 2 samples of the pyramid of Khufu L11 and Pis1. On the opposite numerous samples from the pyramids (about 25 among the 35 ones which were investigated) are very non-homogeneous: one observes inclusions (about 20  $\mu\text{m}$  wide or larger) of Na, Cl and/or S which are correlated with a lack of Ca and O.

#### 4. Discussion

The most abundant chemical compounds beside calcium carbonate are sodium, chlorine and in several ones sulfur compounds. Clusters of aluminum and silicon oxides, often correlated, are present as substitutes of calcium carbonate.

Na and Cl are systematically correlated and could at first sight be interpreted as inclusions of sodium chloride (Figures 8, 9, 10). Nevertheless, the Na signal is always higher than what is needed to form NaCl. In addition, at the sites of high concentrations of Na and Cl, one observes that the Ca and O concentrations are less than in the vicinity. We then conclude that  $\text{Na}_2\text{O}$  (with certainly some  $\text{H}_2\text{O}$ ) is mixed into the NaCl clusters. One has indeed more oxygen atoms in a calcium carbonate than in a hydrated sodium oxide and in water.  $\text{Na}_2\text{O}$  with  $\text{H}_2\text{O}$  suggest the presence of NaOH at some time of the construction which is consistent with the high pH of the ma-

terial already reported by Davidovits (Davidovits, 1986; Davidovits & Morris, 1988) and Barsoum (Barsoum et al., 2006; MacKenzie K. J. D. et al., 2011).

The number of Na and Cl clusters may be small (Figure 8) but sometimes abundant (Figure 9 and figure 10).

The presence of sulphur in several samples is also reported by Barsoum (Barsoum et al., 2006) and Davidovits (Davidovits, 1986; Davidovits & Morris, 1988) who reports that he has found gypsum in several pyramid's samples. This is in accordance with our results, considering samples with high sulfur content, see Tables 1 and 2. Small sulfur clusters are indeed present but are sometimes much larger in other pyramid's samples as shown in Figure 10 where a strong correlation with calcium is observed. On the other hand, sulfur may be also present outside calcium rich regions. Sulfur may be therefore from different origins, one origin may be natron because it is present only in samples containing sodium and chlorine clusters.

Magnesium, phosphorus and potassium are also more present in pyramid samples than in quarries samples, but they are not distributed in clusters. We attribute their presence to the ash used in the binder: in addition to the main parts of calcium and magnesium oxides wooden ashes contain small quantities of oxides of phosphorus, potassium, manganese and iron. The inclusions of Al and Si are also shown in Figure 11.

PIXE and PIGE are atomic and nuclear methods of elemental analysis and are not suitable to give the actual

Table 2

Khufu pyramid outside blocks										
Sample	CaCO <sub>3</sub>	Na <sub>2</sub> O	Cl	SO <sub>3</sub>	MgO	SiO <sub>2</sub>	Al <sub>2</sub> O <sub>3</sub>	K <sub>2</sub> O	P <sub>2</sub> O <sub>5</sub>	FeO
L11	95,13		0,04	2,16	0,41	1,28	0,39			0,2
M2	92,92	0	0,28	1,16	3,63	0,66	0	0	1,1	0,08
M1	72,45	0,53	0,19	1,45	12,96	9,07	2,16	0,26	0	0,57
M4	72,75	0,46	0,16	0,47	16,36	5,96	2,4	0,2	0,1	0,48
<b>MX</b>	<b>66,33</b>	<b>1,01</b>	<b>0,35</b>	<b>3,31</b>	<b>5,02</b>	<b>21,01</b>	<b>1,38</b>	<b>0,19</b>	<b>0,41</b>	<b>0,37</b>
MP	81,21	0,31	0,1	0,13	8,49	8,32	0,36		0,04	0,08
<b>X1</b>	<b>42,33</b>	<b>3,07</b>	<b>1,36</b>	<b>31,96</b>	<b>0,9</b>	<b>11,33</b>	<b>5,23</b>	<b>0,48</b>	<b>0,25</b>	<b>2,33</b>
<b>VT3</b>	<b>87,27</b>	<b>0,96</b>	<b>0,34</b>	<b>1,27</b>	<b>1,28</b>	<b>7,24</b>	<b>0,71</b>	<b>0,13</b>		<b>0,21</b>
<b>VTR3</b>	<b>93,92</b>	<b>1,17</b>	<b>0,42</b>	<b>0,53</b>	<b>0,59</b>	<b>0,41</b>	<b>0,14</b>	<b>0,06</b>	<b>0,78</b>	<b>0,74</b>
<b>VTRS</b>	<b>87,97</b>	<b>3,08</b>	<b>0,88</b>	<b>0,22</b>	<b>0,77</b>	<b>5,13</b>	<b>0,4</b>	<b>0,17</b>	<b>0,36</b>	<b>0,08</b>
FH9	63,68	0,23	0,12	27,24	0,83	4,5	1,91	0,17	0,3	0,53
FH45	88,58	1,58	0,44	0,85	1,58	2,98	1,2	0,13	1,43	0,27
RS16	93,78	0,34	0,1	1,7	0,49	1,65	0,79			0,47
RSH16	64,09		0,07	30,39	0,51	2,74	1	0,11	0,31	0,38
RS14	90,58	0,11	0,15	1	0,71	4,27	1,52	0,1		0,75
<b>BIGVTY</b>	<b>82,12</b>	<b>1,53</b>	<b>0,55</b>	<b>3,85</b>	<b>1,41</b>	<b>6,9</b>	<b>2,11</b>	<b>0,05</b>	<b>0,29</b>	<b>0,56</b>
BVTY2	89,7	0,2	0,02	1,23	0,93	4,63	2,02	0	0	0,63
<b>15B</b>	<b>88,61</b>	<b>0,74</b>	<b>0,23</b>	<b>1,28</b>	<b>1,39</b>	<b>5,98</b>	<b>0,97</b>	<b>0,09</b>		<b>0,12</b>
<b>RSH15</b>	<b>87,4</b>	<b>2,03</b>	<b>0,63</b>	<b>1,76</b>	<b>2,17</b>	<b>3,51</b>	<b>0,59</b>	<b>0,27</b>	<b>0,35</b>	<b>0,18</b>
<b>B15B</b>	<b>88,61</b>	<b>0,53</b>	<b>0,2</b>	<b>1,25</b>	<b>1,29</b>	<b>6,31</b>	<b>1,02</b>	<b>0,11</b>	<b>0</b>	<b>0,13</b>

Khufu pyramid entrance										
Sample	CaCO <sub>3</sub>	Na <sub>2</sub> O	Cl	SO <sub>3</sub>	MgO	SiO <sub>2</sub>	Al <sub>2</sub> O <sub>3</sub>	K <sub>2</sub> O	P <sub>2</sub> O <sub>5</sub>	FeO
Pis1	93,49	0,19	0,07	0,62	0,87	2,6	1,08	0	0,19	0,64
<b>FH6</b>	<b>90,77</b>	<b>0,28</b>	<b>0,22</b>	<b>0,74</b>	<b>0,87</b>	<b>3,81</b>	<b>1,61</b>	<b>0,11</b>	<b>0,28</b>	<b>0,5</b>

Khufu Pyramid Great Gallery										
Sample	CaCO <sub>3</sub>	Na <sub>2</sub> O	Cl	SO <sub>3</sub>	MgO	SiO <sub>2</sub>	Al <sub>2</sub> O <sub>3</sub>	K <sub>2</sub> O	P <sub>2</sub> O <sub>5</sub>	FeO
<b>FH123</b>	<b>87,24</b>	<b>2,02</b>	<b>0,79</b>	<b>0,69</b>	<b>1,15</b>	<b>4,89</b>	<b>1,47</b>	<b>0,22</b>	<b>0,21</b>	<b>0,53</b>
<b>FH7</b>	<b>51,37</b>	<b>2,07</b>	<b>1,08</b>	<b>35,29</b>	<b>0,98</b>	<b>5,57</b>	<b>1,91</b>	<b>0,28</b>	<b>0,28</b>	<b>0,75</b>

Khafra pyramid outside block										
Sample	CaCO <sub>3</sub>	Na <sub>2</sub> O	Cl	SO <sub>3</sub>	MgO	SiO <sub>2</sub>	Al <sub>2</sub> O <sub>3</sub>	K <sub>2</sub> O	P <sub>2</sub> O <sub>5</sub>	FeO
<b>MYKF</b>	<b>84,25</b>	<b>0,56</b>	<b>0,2</b>	<b>0,87</b>	<b>5,14</b>	<b>5</b>	<b>2,16</b>	<b>0,13</b>	<b>0,15</b>	<b>0,91</b>

Table 2: Composition of samples measured by micro-PIXE. Concentrations are expressed as carbonates and oxides in weight-percentages. Significant amount (0.2-0.4 %) of fluorine was detected in some samples.

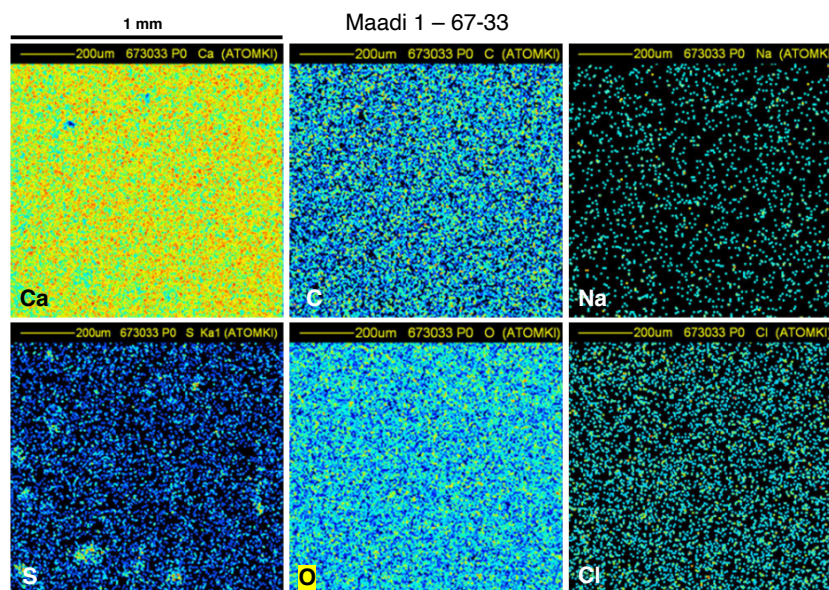


Figure 7: Characteristic X-ray maps of Ca, S, C, O, Na and Cl distribution for a sample collected at Maadi quarry. Similar results were obtained for all samples from Maadi and Turah quarries, for samples of the bedrock of Saqqarah and samples L11 and Pis1 of the pyramid of Khufu. See also data of Table 1.

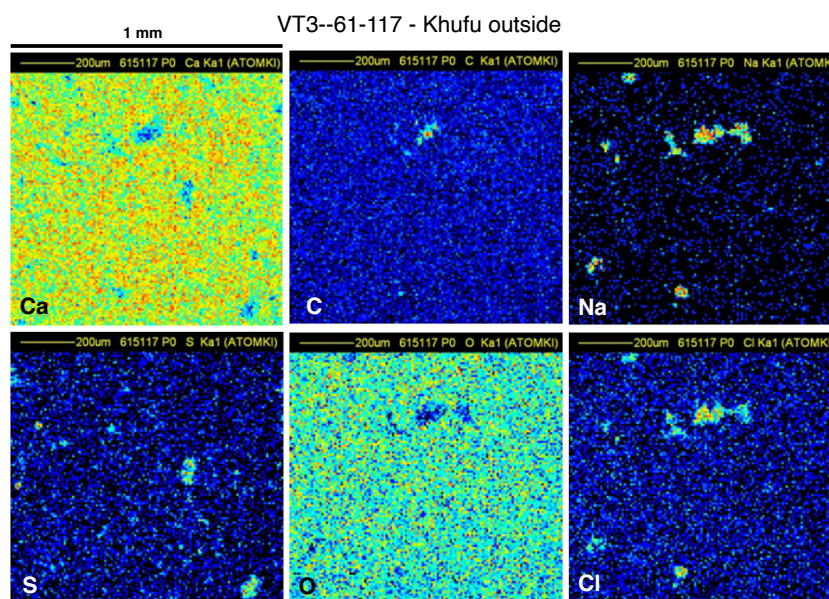


Figure 8: Characteristic X-ray maps of Ca, S, C, O, Na and Cl distribution for sample VT3 collected on the pyramid of Khufu, outside block. Na and Cl inclusions are correlated. Similar results were obtained for other pyramid samples BIGVTY, FH6, Fh123, Mx and MYKF. See also data of Table 1.

chemical composition. Nevertheless, the observation of the maps allows us to suggest the presence of some chemical compounds by looking at localisation of Na, Cl and S relative to the localisation of Ca and O. In particular, the presence of NaCl in pyramid samples only (which I verify in the majority of the analysed samples simply with my tongue!) is chemically explained by the geochemical reaction scheme of Davidovits (Davidovits, 2017) (chapter 6 – p. 43) reproduced in figure 12 (see the end products in steps 3 and 4).

Concerning the presence of sulphur in high concentra-

tion (Figure 10) it is important to point out that Egyptian natron often contains Na-sulfate which causes the formation of hydrated Ca- sulfate, which cannot be easily distinguished from natural gypsum.

The identification of clusters in the maps collected on pyramids samples, showing a high concentration of Na, S and Cl as reported in Figures 9 and 10, but never in the maps related to quarries samples (see figure 5), is in complete agreement with the results of Barsoum (Barsoum et al., 2006) who states that the presence of amorphous microstructures in the pyramid stones (not occurring in

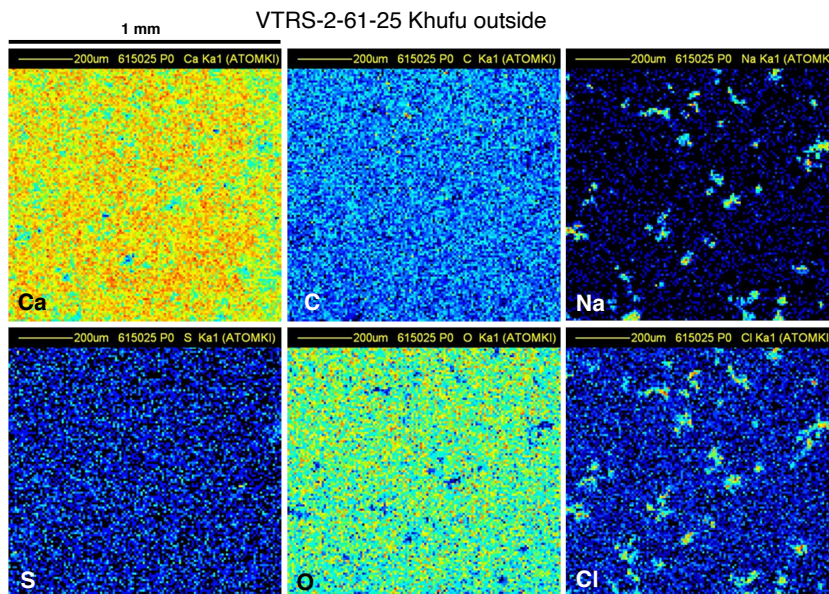


Figure 9: Characteristic X-ray maps of Ca, S, C, O, Na and Cl distribution for sample VTRS collected on the pyramid of Khufu, outside block. Na and Cl inclusions are correlated. Similar results were obtained for other pyramid samples (see also data of Table 1).

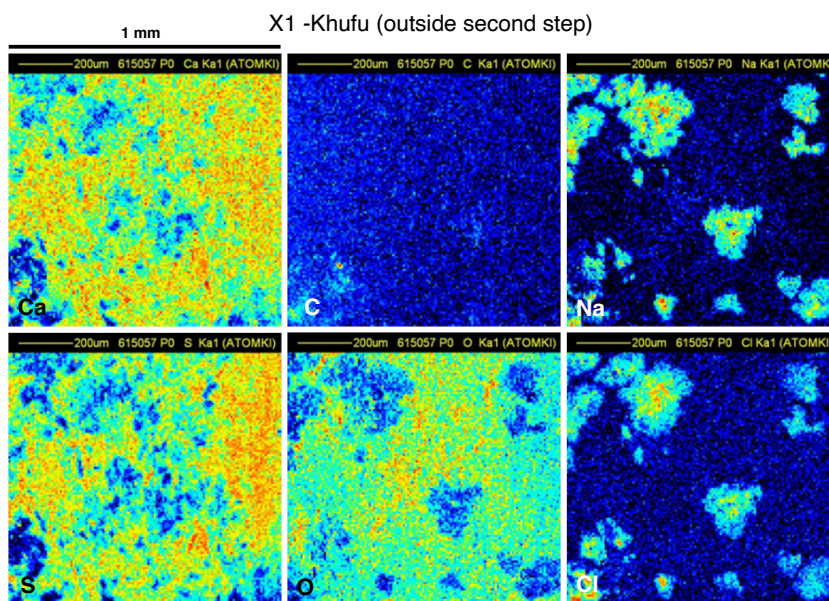


Figure 10: Characteristic X-ray maps of Ca, S, C, O, Na and Cl distribution for sample X1 collected on the pyramid of Khufu, outside block second step. Ca and S, Na and Cl inclusions are correlated. Similar results were obtained for other pyramid samples FH7 and FH9. See also data of Table 1.

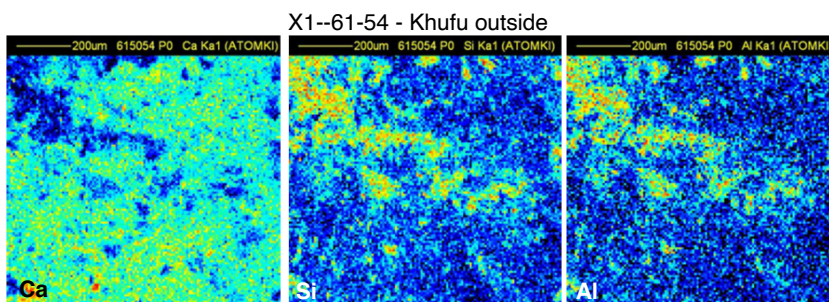


Figure 11: Characteristic X-ray maps of Ca, Si, Al distribution for sample X1 collected on the pyramid of Khufu, outside block. Si and Al inclusions are correlated. Similar results were obtained for other pyramid samples M2, M4 and RS14. See also data of Table 1.

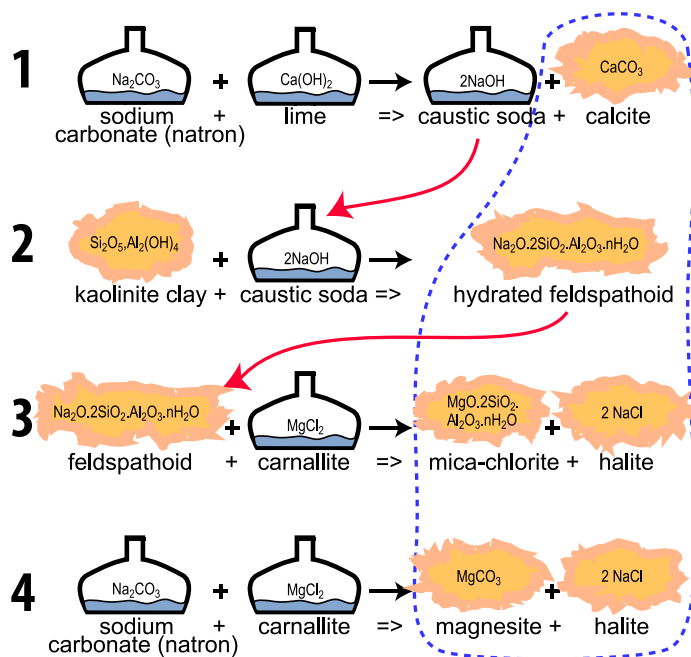


Figure 12: Geochemical reaction scheme for kaolinite clay and limestone from Giza (Egypt), reproduced from Davidovits 2017, page 43.

natural similar materials) indicates that the material was formed in a liquid phase which was solidified in a short time. This short time of solidification was also confirmed by a completely independent method. Advised by our paper of 2009 (Demortier, 2009) Igor Tunyi and Ibrahim A. El-hemaly performed paleo-magnetic investigation of the great Egyptian Pyramids (Khufu and Khafra) and confirm the presence of original oriented ferromagnetic grains which can only be explained if the blocks were cast on site (Túnyi & El-hemaly, 2012).

## 5. Conclusion

The present paper is a continuation of the efforts to critically investigate the construction technique of the great pyramids at Giza. Previous studies have shown that Davidovits' method suggesting the use of the agglomeration technique applying limestone, pebbles and natron is by far the most plausible. Qualitative PIGE, PIXE and structural characterization by NMR-spectroscopy accomplished a decade ago revealed the presence of F, Na, Mg, Al, Si (PIGE), Ca, Sr, As and other elements (PIXE) as well as the presence of a geopolymer binding material (NMR).

The quantitative micro-PIXE analyses carried out on a large scale of samples collected from different sites of the Khufu and Khafra pyramids as well as from neighbouring Egyptian quarries give creditable evidences on the new ideas referring to the construction techniques of the pyramids. While X-ray maps of the quarry samples are rather homogenous or contain only fine (natural) inclusions (aluminium, silicon and/or iron oxides), those of the

pyramid samples show coarse heterogeneities. The major components of the pyramid samples are calcium carbonates/sulphates, Na and Cl-containing additives (natron) and silicates. These new analytical results confirm that blocks were not natural limestone but really moulded on site and not hewn as it was generally stated.

These investigations embodied by a multidisciplinary team have shown the importance and complementary character of the applied analytical procedures to solve the "Mystery of the Pyramids". Many questions raised by these investigations are perspective to be further analytical studied, *e.g.* the importance of trace elements.

## Acknowledgements

I am indebted to the scientific and technical staffs of LARN (Namur- Belgium), CEDAD (Lecce — Italy) and ATOMKI (Debrecen — Hungary) for their important support during the long runs of measurements. My special thanks to Prof. Á.Z. Kiss and Dr. I. Uzonyi for the helpful discussions and their valuable suggestions concerning the experiment and manuscript.

## Notes added by the editor

### Note n°1 on the provenience of the samples

It is well known that the Egyptian Authorities are always rejecting any research proposal which requires the collecting of samples from the Great Pyramids. They never gave any valid explanation for their action. Therefore, all scientific analysis which have been carried out and published by materials scientists during the last four decades, since 1980, were relying on "non-authorized" samples. We asked Guy Demortier to explain how he got the numerous samples which constitute now his private collection. His answer is:

"... Provenience: I had 3 samples in 1989. (...) That's all I had before the publication of my first paper released in 2004. Subsequently, when I presented results on these 3 samples to illustrate PIXE-PIGE-RBS applications concerning archaeological objects, in conferences, I suggested that participants bring me samples if they had the possibility of taking some on the occasion of their possible visit to Giza. I have been to Cairo only once as guest speaker for a talk on the welding of gold in antiquity, in 1990, and when I visited the site I asked if I could take a few  $\text{cm}^3$  of sample myself. I was then told that it was impossible to get the smallest fragment out of Egypt. So I have no samples taken by myself. I received thirty pieces between 1995 and 2015, all unofficially taken by a wide variety of scientists: (10 people including 7 Belgian) physicists, chemists, engineer, geologist, geographer, biologist, egyptologist. The



vast majority, and especially the egyptologist, asked for anonymity and I promised everyone not to reveal their identity. The size ranges from a few grams to more. For microanalyses, I always took an internal fragment (to avoid any pollution) to make a pellet with a polished face to carry out the scan."

#### Note n°2 during the peer-reviewing process

Hundreds of thousands of people have read articles and seen videos on the internet dealing with the pyramids of Egypt having been constructed from geopolymer concrete. The contra-arguments of the opponents are always based on the same papers written by American geologists, published 15 to 30 years ago. These three publications are draped in scientific impartiality when this is not the case. The most cited study shown in the videos at YouTube is the analysis carried out on the "Lauer Sample" by the American petrologist Dipayan Jana, published in 2007 and titled: "Evidence from detailed petrographic examinations of casing stones from the great pyramid of khufu, a natural limestone from tura, and a man-made (Geopolymeric) limestone", *Proceedings of the 29th Conference of Cement Microscopy*, Quebec, Canada, May 20-24 (2007), pp. 207-266. He strongly criticized our original study. We have recently discovered that Jana's study was performed on a fake "Lauer Sample", not on the genuine archaeological material. This "fake Lauer-Sample" was a simple piece of limestone from Turah sent to Dipayan Jana by one of these American geologists. Unfortunately, critics ignoring this forgery and relying on said papers persist by pointing out these three geological studies as the ones that restore the truth. Jana's study of the rock passed off as the "Lauer Sample" can no longer serve as a reference.

#### References

- Barsoum, M., Ganguly, A., & Hug, G. (2006). Microstructural Evidence of Reconstituted Limestone Blocks in the Great Pyramids of Egypt. *Journal of the American Ceramic Society*, 89(12), 3796–3788.
- Davidovits, J. (1986). X-Rays Analysis and X-Rays Diffraction of Casing Stones from the Pyramids of Egypt, and the Limestone of the Associated Quarries. In A. Rosalie David (Ed.), *Science in Egyptology* (pp. 511–520). Manchester: Manchester University Press.
- Davidovits, J. (2017). *Why the Pharaohs built the pyramids with fake stones*. Institut Géopolymère. ISBN: 97829514822043.
- Davidovits, J. & Morris, M. (1988). *The pyramids, an enigma solved*. New-York: Hippocrene books. ISBN: 087052559X.
- Demortier, G. (1995). Analysis of light elements with a nuclear microprobe — A review. *Nuclear Instruments and Methods in Physics Research. Section B: Beam Interactions with Materials and Atoms*, 104(1/4), 244–254.
- Demortier, G. (2004). PIXE, PIGE and NMR study of the masonry of the pyramid of Cheops at Giza. *Nuclear instruments and methods in physics research. Section B: Beam interactions with materials and atoms*, 226, 98–109.
- Demortier, G. (2009). Revisiting the construction of the Egyptian pyramids. *Europhysics News*, 40(1), 27–31.
- Demortier, G., Quarta, G., Butalag, K., D'Elia, M., & Calcagnile, L. (2008). Benefits of combined PIXE and AMS with new accelerators. *XRS X-Ray Spectrometry*, 37(2), 178–183.
- Grime, G. W. (2017). High-Energy Ion Beam Analysis & Proton Microprobe (Method and Background). In J. C. Lindon, G. E. Tranter, & D. W. Koppenaal (Eds.), *Encyclopedia of Spectroscopy and Spectrometry* (pp. 103–121 & 785–788). Oxford: Academic Press, third edition.
- Grime, G. W., Dawson, M., Marsh, M., McArthur, I. C., & Watt, F. (1991). The Oxford submicron nuclear microscopy facility. *Nuclear Instruments and Methods in Physics Research Section B: Beam Interactions with Materials and Atoms*, 54(1-3), 52–63.
- Hoskin, P. W. O. (1999). SIMS Determination of  $\mu\text{g g}^{-1}$ -Level Fluorine in Geological Samples and its Concentration in NIST SRM 610. *Geostandards and Geoanalytical Research*, 23(1), 69–76. DOI: 10.1111/j.1751-908X.1999.tb00560.x.
- Kiss, Á. Z., Koltay, E., Nyakó, B., Somorjai, E., Anttila, A., & Räsänen, J. (1985). Measurements of relative thick target yields for PIGE analysis on light elements in the proton energy interval 2.4-4.2 MeV. *Journal of Radioanalytical and Nuclear Chemistry*, 89(1), 123–141.
- Koltay, E., Pászti, F., & Kiss, Á. Z. (2011). Chemical Applications of Ion Accelerators. In A. Vértes, S. Nagy, Z. Klencsár, R. Lovas, & F. Rösch (Eds.), *Handbook of Nuclear Chemistry*, number 3 in Springer reference (pp. 1695–1735). Hamburg: Springer Verlag.
- MacKenzie K. J. D., Smith M. E., Wong A., Hanna J. V., Barry B., & Barsoum M. W. (2011). Were the casing stones of Senefru's Bent Pyramid in Dahshour cast or carved? Multinuclear NMR evidence. *Materials Letters*, 65(2), 350–352.
- Rajta, I., Borbély-Kiss, I., Móri, G., Bartha, L., Koltay, E., & Kiss, Á. (1996). The new ATOMKI scanning proton microprobe. *Nuclear Instruments and Methods in Physics Research Section B: Beam Interactions with Materials and Atoms*, 109-110, 148–153.
- Szabó, G. & Borbély-Kiss, I. (1993). PIXYKLM computer package for PIXE analyses. *Nuclear Instruments and Methods in Physics Research Section B: Beam Interactions with Materials and Atoms*, 75(1-4), 123–126.
- Túnyi, I. & El-hemaly, I. A. (2012). Paleomagnetic investigation of the great egyptian pyramids. *Europhysics News*, 43(6), 28–31.
- Uzonyi, I., Rajta, I., Bartha, L., Kiss, A. Z., & Nagy, A. (2001). Realization of the simultaneous micro-PIXE analysis of heavy and light elements at a nuclear microprobe. *Nuclear Instruments and Methods in Physics Research Section B*, 181(1-4), 193–198.
- Uzonyi, I. & Szabó, G. (2005). PIXEKLM-TPI - a software package for quantitative elemental imaging with nuclear microprobe. *Nuclear Instruments and Methods in Physics Research Section B: Beam Interactions with Materials and Atoms*, 231(1-4), 156–161.
- Wagner, B., Nowak, A., Bulska, E., Hametner, K., & Günther, D. (2012). Critical assessment of the elemental composition of Corning archeological reference glasses by LA-ICP-MS. *Analytical and Bioanalytical Chemistry*, 402(4), 1667–1677. DOI: 10.1007/s00216-011-5597-8.